



## Flow field, heat transfer and entropy generation of nanofluid in a microchannel using the finite volume method

Majid Kerdarian and Ehsan Kianpour\*

Department of Mechanical Engineering, Najafabad Branch, Islamic Azad University, Najafabad, Iran

### Article info:

Received: 16/10/2016

Accepted: 13/06/2018

Online: 17/06/2018

### Keywords:

Entropy generation,  
Microchannel,  
Slip velocity,  
Temperature jump,  
Cu-water nanofluid.

### Abstract

In this study, the finite volume method and the SIMPLER algorithm is employed to investigate forced convection and entropy generation of Cu-water nanofluid in a parallel plate microchannel. There are four obstacles through the microchannel, and the slip velocity and temperature jump boundary conditions are considered in the governing equations to increase the accuracy of modeling. The study is conducted for the Reynolds numbers in the range of  $0.1 < Re < 10$ , Knudsen numbers ranging of  $0 < Kn < 0.1$ , and volume fraction of nanoparticles ranging of  $0 < \phi < 0.04$ . The results show that by increasing the Knudsen number, the average Nusselt number and total entropy generation rate decrease. Moreover, with augmentation of the Reynolds number, the average Nusselt number and total entropy generation rate decrease. What's more, by increasing the volume fraction of nanofluids, the temperature of the nanofluid reduces, and as a result, the temperature gradient as well as heat transfer increase.

### Nomenclature

$c_i$	Coefficients of fully developed velocity profile	$\dot{S}'''$	Dimensionless volumetric rate of entropy generation
$c_p$	Specific heat capacity (J/kg K)	$\dot{S}$	Dimensionless total rate of entropy generation
$D_h$	Hydraulic diameter (m)	$T$	Temperature (K)
$h$	Local heat transfer coefficient (W/m <sup>2</sup> K)	$(u, v)$	Velocity components (m/s)
$k$	Thermal conductivity (W/m K)	$(U, V)$	Dimensionless velocity components
Kn	Knudsen number	$(x, y)$	Coordinates (m)
$L$	Unit length (m)	$(X, Y)$	Dimensionless coordinates
$n$	Unit normal vector		
Nu	Nusselt number		
$p$	Pressure (N/m <sup>2</sup> )		
$P$	Dimensionless pressure		
Po	Poiseuille number ( $\equiv f Re$ )		
Pr	Prandtl number		
Re	Reynolds number		
$\dot{S}'''$	Volumetric rate of entropy generation		
		<b>Greek symbols</b>	
		$\alpha$	Thermal diffusivity (m <sup>2</sup> /s)
		$\gamma$	Heat capacity ratio ( $\equiv c_p/c_v$ )
		$\theta$	Dimensionless temperature
		$\lambda$	Mean free path (m)
		$\mu$	Dynamic viscosity (kg/m s)
		$\nu$	Kinematic viscosity (m <sup>2</sup> /s)

\*Corresponding author

email address: ekianpour@pmc.iaun.ac.ir

$\rho$	Density (kg/m <sup>3</sup> )
$\chi$	Irreversibility distribution ratio
$\phi$	Nanoparticles volume fraction

**Subscripts**

$0$	Reference state value
$av$	Average
$bf$	Base fluid
$eff$	Effective
$fd$	Fully developed region
$h$	Hot walls
$in$	Inlet flow
$nf$	Nanofluid
$np$	Nanoparticles
$static$	Static component of thermal conductivity
$w$	Walls

**1. Introduction**

With the development of science and technology, people began to realize that with the size decreasing the system will own many advantages that do not appear in conventional size, including compact size, disposability, and cooling system for electronic devices to various microscale electromechanical systems, such as micropumps and microturbines [1]. Microchannels, however, are basic structures in these systems. The Knudsen number (Kn), defined as the ratio of molecular mean free path length to a representative physical length scale, can be in the range  $0.001 < Kn < 0.1$ . Based on this number, the flow in microchannels are classified into four flow regimes of continuum flow ( $Kn < 0.001$ ), slip flow ( $0.001 < Kn < 0.1$ ), transition flow ( $0.1 < Kn < 10$ ), and free molecular flow ( $Kn > 10$ ). The flow in the most application of these systems, such as micro-gyroscope, accelerometer, flow sensors, micronozzles, microvalves, is in slip flow regime, which is characterized by slip flow at the wall. Traditionally, the no-slip condition at the wall is enforced in the momentum equations and an analogous no-temperature-jump condition is applied in the energy equation. Strictly speaking, no-slip/no-jump boundary conditions are valid only if the fluid flow adjacent to the surface is in thermodynamic equilibrium. This requires an infinitely high frequency of collisions between the fluid and the solid surface [1, 2]. In practice, the no-slip/no-jump condition leads to

reasonably accurate predictions as long as  $Kn < 0.001$ . Beyond that, flow in devices shows significant slip since characteristic length is on the order of the mean free path of the fluid or gas molecules. It means that the collision frequency is simply not high enough to ensure equilibrium and a certain degree of tangential velocity slip and temperature jump must appear. Slip velocity at the wall is the most important feature in micro/nanoscale that differs from the conventional internal flow. Therefore, the characteristics of slip flow are very important for designing and optimizing the micro/nano systems. Numerous researches were dedicated to the use of microchannel and nanofluids in industrial and engineering problems over the past few years [3-11]. As early as 1981 and for the first time, Tuckerman and Pease [12] scrutinized meticulously fluid flow and heat transfer in micro-scaled size. Yu and Ameel [13, 14] studied laminar slip-flow forced convection under thermally developing flow for constant wall temperature and isoflux boundary conditions. The energy equation was solved analytically using the integral transform technique, neglecting axial conduction and the heat transfer augmentation, as the rarefaction was studied. Renksizbulut et al. [15] solved slip-flow and heat transfer in the entrance region of rectangular microchannels for the cases in which Prandtl number equals to unity. Forced convection fluid flow and heat transfer of Al<sub>2</sub>O<sub>3</sub>-water nanofluid in a two-dimensional rectangular microchannel were examined by Akbarinia et al. [16]. In order to enhance heat transfer, they added nanoparticles to the base fluid at low Reynolds numbers. They demonstrated that the maximum increment of the Nusselt number in constant Reynolds numbers is not due to the increase in nanoparticles concentration, but to the increase in the inlet velocity, to reach a constant Reynolds number. Very recently, Karimipour [17] conducted a numerical simulation to study forced convection heat transfer of water-Ag, water-Cu and water-Al<sub>2</sub>O<sub>3</sub> nanofluids in a microchannel. He considered the slip velocity and temperature jump boundary conditions and correlated a new relation predicting the nanofluid Nusselt number. Based on his results,

higher values of slip coefficient correspond to more temperature jump and slip velocity and less Nusselt number.

One of the important objectives of thermal systems engineering is to analyze the utilization of thermal energy in an efficient manner. From the viewpoint of thermodynamics, the decrease of entropy generation means the decrease of irreversibility and less loss of exergy. Therefore, in the energy optimization problems and design of many traditional heat removal engineering devices, it is necessary to evaluate the entropy generation or exergy destruction due to heat transfer and viscous friction as a function of the physical and geometrical parameters selected for the optimization analysis. This procedure, known as the Entropy Generation Minimization (EGM) method [18, 19], is a thermodynamic approach to optimization of engineering systems for higher energy efficiency. Hooman [20] investigated forced convection heat transfer and entropy generation in micro-electro-mechanical systems in the slip-flow regime. He considered two kinds of cross-sections, parallel plates, and micro-pipe. He also evaluated the effects of temperature jump, viscosity dissipation and geometric parameters on flow field and heat transfer. Haddad et al. [21] numerically investigated the entropy generation due to steady laminar forced convection fluid flow through parallel plates microchannel. They found that the entropy generation within the microchannel decreases as Knudsen number increases, and increases as Reynolds, Prandtl, Eckert numbers and the nondimensional temperature difference increase. Also, the contribution of the viscous dissipation in the total entropy generation increases as Knudsen number increases over wide ranges of the flow controlling parameters. Pourmahmoud et al. [22] performed a numerical simulation to study flow field, heat transfer and entropy generation in an internally ribbed microchannel using finite volume method. They examined the impact of parameters such as Reynolds number, heat flux and rib height on entropy generation. They observed that the Reynolds number and wall heat flux control the optimum rib height and minimum total entropy generation rate.

The aim of the present investigation is to study flow field, heat transfer and entropy generation of Cu-water nanofluid through a microchannel with obstacles by considering slip velocity and temperature jump boundary conditions. In order to solve the governing equations, the finite volume method is applied. Due to small dimensions of microchannel and as a result, the small value of its characteristic length, the Reynolds number is usually less than 10, and the Knudsen number is also considered between  $10^{-3}$  and 0.1 as far as in this interval the hypothesis of slip flow regime is true (0 and 0.1 are limitation factors).

### 2. Problem formulation

The geometry of microchannel is depicted in Fig. 1. The proportion of the length to the height of the microchannel is ten.  $D_h = 2 \times 0.5L = L$  and the height of the microchannel is equal to half of the unit length. The cold inlet flow is hydrodynamically fully developed. Both top and bottom plates are hot, and the slip velocity and temperature jump boundary conditions are applied on them. Furthermore, four hot obstacles are placed inside the microchannel. The microchannel is filled with Cu-water nanofluid. Moreover, the nanofluid is considered Newtonian and incompressible. Thermo-physical properties of water as a base fluid and Cu nanoparticles are presented in Table 1.

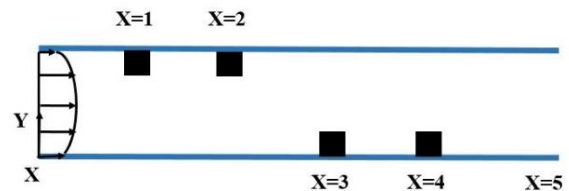


Fig. 1. The schematic of the problem.

Table 1. Thermo-physical properties of base fluid (in 300 K) and nanoparticles [23].

	$\rho$ (kg/m <sup>3</sup> )	$C_p$ (J/kg. K)	$K$ (W/m. K)	$B$ (1/K)	$D$ (nm)
Water	997.1	4179	0.613	$2.1 \times 10^{-4}$	<b>0.278</b>
Cu	8933	385	401	$1.67 \times 10^{-5}$	-

The conservation of mass, momentum and energy equations for the two-dimensional, steady, and laminar forced convection of the nanofluid flow are as follows [16]:

$$\frac{\partial}{\partial x}(\rho_{nf}u) + \frac{\partial}{\partial y}(\rho_{nf}v) = 0 \tag{1}$$

$$\frac{\partial}{\partial x}(uu) + \frac{\partial}{\partial y}(vu) = -\frac{1}{\rho_{nf}} \frac{\partial p}{\partial x} + \frac{\partial}{\partial x}\left(v_{nf} \frac{\partial u}{\partial x}\right) + \frac{\partial}{\partial y}\left(v_{nf} \frac{\partial u}{\partial y}\right) \tag{2}$$

$$\frac{\partial}{\partial x}(uv) + \frac{\partial}{\partial y}(vv) = -\frac{1}{\rho_{nf}} \frac{\partial p}{\partial y} + \frac{\partial}{\partial x}\left(v_{nf} \frac{\partial v}{\partial x}\right) + \frac{\partial}{\partial y}\left(v_{nf} \frac{\partial v}{\partial y}\right) \tag{3}$$

$$\frac{\partial}{\partial x}(uT) + \frac{\partial}{\partial y}(vT) = \frac{\partial}{\partial x}\left(\alpha_{nf} \frac{\partial T}{\partial x}\right) + \frac{\partial}{\partial y}\left(\alpha_{nf} \frac{\partial T}{\partial y}\right) \tag{4}$$

where  $u$  and  $v$  are the velocity components in the  $x$  and  $y$  directions, respectively.  $\rho$  is the fluid density,  $\mu$  is the dynamic viscosity,  $c_p$  is heat capacity at constant pressure and  $k$  is the thermal conductivity.

The volumetric rate of entropy generation is evaluated from the following equation [24]:

$$s''' = \frac{k_{nf}}{T_0^2} \left[ \left(\frac{\partial T}{\partial x}\right)^2 + \left(\frac{\partial T}{\partial y}\right)^2 \right] + \frac{\mu_{nf}}{T_0} \left[ 2 \left\{ \left(\frac{\partial u}{\partial x}\right)^2 + \left(\frac{\partial v}{\partial y}\right)^2 \right\} + \left(\frac{\partial u}{\partial y} + \frac{\partial v}{\partial x}\right)^2 \right] \tag{5}$$

in which  $T_0 = (T_h + T_{in})/2$ .

The governing equations are casted into the dimensionless form by using the following dimensionless parameters:

$$(X, Y) = \frac{(x, y)}{D_h}; D_h = 2H; \tag{6}$$

$$(U, V) = \frac{(u, v)}{u_{in}}; P = \frac{p}{\rho_{nf}u_{in}^2}$$

$$\theta = \frac{T - T_{in}}{\Delta T}; \Delta T = T_h - T_{in};$$

$$Re = \frac{u_{in}D_h}{\nu_{bf}}; Pr = \frac{\nu_{bf}}{\alpha_{bf}}$$

where  $D_h$  is the hydraulic diameter of the microchannel and  $\Delta T = T_h - T_{in}$ . Hence, the non-dimensionalized governing equations alter as follow by using the foregoing dimensionless variables:

$$\frac{\partial}{\partial X}\left(\frac{\rho_{nf}}{\rho_{bf}}U\right) + \frac{\partial}{\partial Y}\left(\frac{\rho_{nf}}{\rho_{bf}}V\right) = 0 \tag{7}$$

$$\frac{\partial}{\partial X}(UU) + \frac{\partial}{\partial Y}(VU) = -\frac{\partial P}{\partial X} + \tag{8}$$

$$\frac{1}{Re} \left[ \frac{\partial}{\partial X}\left(\frac{v_{nf}}{v_{bf}} \frac{\partial U}{\partial X}\right) + \frac{\partial}{\partial Y}\left(\frac{v_{nf}}{v_{bf}} \frac{\partial U}{\partial Y}\right) \right] + \frac{\partial}{\partial X}(UV) + \frac{\partial}{\partial Y}(VV) = -\frac{\partial P}{\partial Y} + \tag{9}$$

$$\frac{1}{Re} \left[ \frac{\partial}{\partial X}\left(\frac{v_{nf}}{v_{bf}} \frac{\partial V}{\partial X}\right) + \frac{\partial}{\partial Y}\left(\frac{v_{nf}}{v_{bf}} \frac{\partial V}{\partial Y}\right) \right] + \frac{\partial}{\partial X}(U\theta) + \frac{\partial}{\partial Y}(V\theta) = \frac{1}{RePr} \left[ \frac{\partial}{\partial X}\left(\frac{\alpha_{nf}}{\alpha_{bf}} \frac{\partial \theta}{\partial X}\right) + \frac{\partial}{\partial Y}\left(\frac{\alpha_{nf}}{\alpha_{bf}} \frac{\partial \theta}{\partial Y}\right) \right] \tag{10}$$

and

$$\dot{S}_{gen}''' = \dot{S}_{gen}''' \frac{T_0^2 D_h^2}{k_{bf} \Delta T^2} = \frac{k_{nf}}{k_{bf}} \left[ \left(\frac{\partial \theta}{\partial X}\right)^2 + \left(\frac{\partial \theta}{\partial Y}\right)^2 \right] + \chi \frac{\mu_{nf}}{\mu_{bf}} \left[ 2 \left\{ \left(\frac{\partial U}{\partial X}\right)^2 + \left(\frac{\partial V}{\partial Y}\right)^2 \right\} + \left(\frac{\partial U}{\partial Y} + \frac{\partial V}{\partial X}\right)^2 \right] \tag{11}$$

The Reynolds and Prandtl numbers are defined, respectively, as:

$$Re = \frac{u_{in} D_h}{\nu_{bf}}; \quad Pr = \frac{\nu_{bf}}{\alpha_{bf}} \tag{12}$$

$$\chi = \frac{\mu_{bf} T_0}{k_{bf}} \left( \frac{u_{in}}{\Delta T} \right)^2 \tag{13}$$

where  $\chi$  is the irreversibility distribution ratio and is assumed  $10^{-3}$  in this study [25].

The boundary conditions of the nanofluid flow with regard to the slip velocity and temperature jump on all of the walls can be expressed as follows [16]:

$$U - U_w = \left( \frac{2 - \sigma_v}{\sigma_v} \right) Kn \frac{\partial U}{\partial Y} \Big|_w \tag{14}$$

$$\theta - \theta_w = \left( \frac{2 - \sigma_T}{\sigma_T} \right) \left( \frac{2\gamma}{\gamma + 1} \right) \tag{15}$$

$$\frac{1}{Pr} \left[ Kn \left( \frac{\partial \theta}{\partial Y} \Big|_w \right) \right]$$

where  $\theta_w = 1$  and  $U_w = 0$ ; and the coefficient value of  $(\sigma_v, \sigma_T, \gamma)$  in most of the engineering applications are equal to one. It is noteworthy that the other terms in complete forms of Eqs. (14 and 15) are neglected [16]. So, the simplified boundary conditions are:

$$U = Kn \frac{\partial U}{\partial Y} \Big|_w \tag{16}$$

$$\theta = \frac{Kn}{Pr} \frac{\partial \theta}{\partial Y} \Big|_w + 1 \tag{17}$$

In order to apply the hydrodynamically fully developed flow at an inlet, the velocity profile at the inlet is presumed as follows:

$$U(Y) = c_1 Y^2 + c_2 Y + c_3 \tag{18}$$

The slip velocity on the boundaries should be imposed on Eq. (18), and the volumetric flow rate at the inlet should be equal to the case in which the uniform velocity ( $U_{uniform} = 1$ ) is assumed at the inlet. So, the considered velocity profile should satisfy the following constraints:

$$U(0) = Kn \frac{\partial U}{\partial Y} \Big|_{Y=0} \tag{19}$$

$$U(0.5) = -Kn \frac{\partial U}{\partial Y} \Big|_{Y=0.5}$$

$$\int_0^{0.5} U(Y) dY = \int_0^{0.5} (1) dY = 0.5$$

By applying the foregoing constraints on Eq. (18), the hydrodynamically fully developed velocity profile becomes:

$$U(Y) = \frac{12}{12Kn + 1} (-2Y^2 + Y + Kn) \tag{20}$$

The density, the heat capacity, the thermal expansion coefficient, the effective dynamic viscosity, and the effective thermal conductivity [26] of the nanofluid are obtained from the following:

$$\rho_{nf} = 1001.064 + 2738.6191\phi - 0.2095T \tag{21}$$

$$0 \leq \phi \leq 0.04, \quad 5 \leq T (\text{°C}) \leq 40$$

$$(c_p)_{nf} = \frac{(1 - \phi)(\rho c_p)_{bf} + \phi(\rho c_p)_{np}}{\rho_{nf}} \tag{22}$$

$$\beta_{nf} = \left( -0.479\phi + 9.3158 \times 10^{-3} T - \frac{4.7211}{T^2} \right) \times 10^{-3} \tag{23}$$

$$0 \leq \phi \leq 0.04, \quad 10 \leq T (\text{°C}) \leq 40$$

$$\mu_{nf} = -0.4491 + \frac{28.837}{T} + 0.574\phi \tag{24}$$

$$-0.1634\phi^2 + 23.053 \frac{\phi^2}{T^2} + 0.0132\phi^3$$

$$-2354.735 \frac{\phi}{T^3} + 23.498 \frac{\phi^2}{d_{np}^2} - 3.0185 \frac{\phi^3}{d_{np}^2}$$

$$1\% \leq \phi \leq 9\%, \quad 20 \leq T (\text{°C}) \leq 70$$

$$, \quad 13 \leq d_{np} (nm) \leq 131$$

$$\frac{k_{nf}}{k_{bf}} = 0.9843 + 0.398\phi^{0.7383} \tag{25}$$

$$\left( \frac{1}{d_{np} (nm)} \right)^{0.2246} \left( \frac{\mu_{nf}(T)}{\mu_{bf}(T)} \right)^{0.0235} -$$

$$3.9517 \frac{\phi}{T} + 34.034 \frac{\phi^2}{T^3} + 32.509 \frac{\phi}{T^2}$$

$$0\% \leq \phi \leq 10\%, \quad 20 \leq T (\text{°C}) \leq 70,$$

$$11 \leq d_{np} (nm) \leq 150$$

Khanafer and Vafai model [26] is used in a wide range of nanoparticle diameter  $13\text{ nm} \leq d_p \leq 131\text{ nm}$ , volume fraction  $1\% \leq \phi_p \leq 9\%$  and temperature  $20 \leq T (^{\circ}\text{C}) \leq 70$ .

The total entropy generation rate can be expressed as follows:

$$\dot{S} = \int_V \dot{S}'' dV \tag{30}$$

The local Nusselt number is obtained from the following equation:

$$\text{Nu} = - \left( \frac{k_{nf}}{k_{bf}} \right) \frac{\partial \theta}{\partial n} \Big|_w \tag{31}$$

where  $n$  is the direction of the outward normal to the wall. The average Nusselt number which is obtained by integrating from Eq. (31) along the hot surfaces, is:

$$\text{Nu}_{av} = \frac{1}{2 \times 5} \int_0^5 (\text{Nu}|_{r=0} + \text{Nu}|_{r=0.5}) dX \tag{32}$$

### 3. Numerical implementation

Governing equations are solved numerically using the finite volume method and SIMPLER algorithm. At first, a finite difference mesh is generated in the solution domain, and then a control volume is created around each node. Then a uniform rectangular staggered grid is generated over the whole computational domain. Subsequently, the governing equations are integrated over each control volume, and by discretizing them, sets of coupled non-linear differential equations are obtained. The set of discretized equations are solved using a line-by-line TDMA solver. This iterative procedure is continued until the relative difference between the residuals of two consecutive iterations for all pressure, temperature; and velocities becomes less than  $10^{-6}$ . Both of the convective and diffusive fluxes of each control volume are merged using a power-law differencing scheme.

#### 3.1. Independence results from grid

In order to find an appropriate grid that leads to the independence results from the grid, the entropy generation for Cu-water nanofluid convection in the microchannel for the grid with various number points obtained are presented in Table 2. Based on the obtained entropy generation values, the number of grid points is  $361 \times 131$ .

**Table 2.** Entropy generation in different grid sizes.

Grid size	$\dot{S}_{gen}$	Relative difference	Grid size	$\dot{S}_{gen}$	Relative difference
$441 \times 121$	18.623	-	$321 \times 131$	-	18.974
$441 \times 131$	18.785	0.86	$361 \times 131$	1.05	18.777
$441 \times 141$	18.945	0.84	$401 \times 131$	0.12	18.754

#### 3.2. Validation of results

To validate the computer program results, some cases of Renksizbulut et al. [15] and Akbarnia et al. [27] studies are simulated using the present program, and their results are compared in Table 3 and Fig. 2. In Table 3, the Poiseuille numbers ( $fRe$ ) in the fully developed region are compared to those of Renksizbulut et al. [15] study for different Knudsen numbers and the local Nusselt number are compared between the present study and literature (Fig. 2). As can be observed from Fig. 2 and Table 3, an excellent conformity exists between the present simulation and those of Renksizbulut et al. [15] and Akbarnia et al. [27] which certifies modeling results accuracy.

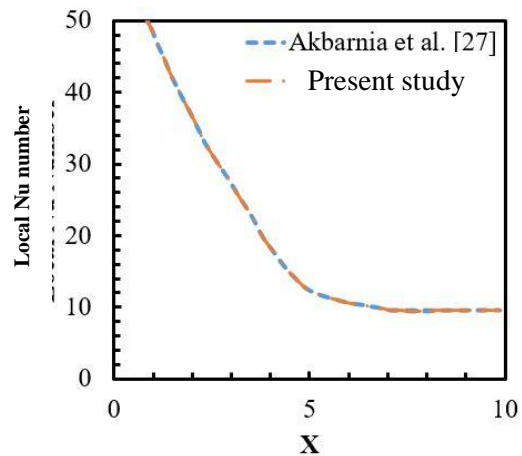


**Fig. 2.** Local Nusselt number comparison between the present study and Akbarnia et al. [27] in  $Re=10$  and  $Kn=0.01$ .

**Table 3.** Friction factors comparison between the present study and Renksizbulut et al. [15] in Re=10 and different Knudsen numbers.

Knudsen numbers	Renksizbulut et al. [15]	Present study	Relative difference with Renksizbulut et al. [15] (%)
0	23.87	23.995	0.52
0.005	22.54	22.637	0.43
0.01	21.33	21.425	0.45
0.025	18.39	18.459	0.38
0.05	14.95	14.998	0.32
0.1	10.88	10.908	0.26

**4. Results and discussion**

In the present study, flow field, heat transfer, and entropy generation are examined in a microchannel filled with Cu-water nanofluid. The slip velocity and temperature jump boundary conditions are also considered in governing equations. Moreover, the effects of different parameters such as Reynolds number, the volume fraction of nanoparticles, and Knudsen number on the average Nusselt number and the total entropy generation rate are evaluated. This study was conducted for Re = 0.1, 3, 7 and 10,  $\phi = 0, 0.01, 0.02, 0.03$  and 0.04, and Kn = 0, 0.035, 0.07 and 0.

*4.1. Streamlines, isothermal, and constant generated entropy lines*

In Fig. 3, streamlines, isothermal, and constant generated etropy lines are depicted in Kn=0.1,  $\phi = 0.03$ , and in different Reynolds numbers. As can be seen in this figure, in Re=0.1, there is a hot region in terms of temperature all over the microchannel as far as the viscosity forces are dominant in this region compared to the inertia forces. Therefore, at the beginning of the microchannel an intense temperature gradient is observed, and after that, the temperature becomes constant. Over the top and bottom hot wall the vertical temperature gradient is very low nearly all over the microchannel, and as a result, the rate of heat transfer is low. Generally, by increasing the Reynolds number, the temperature gradient over the hot surfaces increases and as a result, the heat transfer rate augments. Moreover, as the Reynolds number increases, over the obstacles, the accumulation

of the streamlines increases, and as a result, the velocity of the flow increases significantly in these regions. In Re=10, the isothermal lines are extended to the end of the microchannel. Furthermore, over the obstacles, the isotherms are heaped up due to augmentation of fluid velocity in these zones, and therefore, the heat transfer on the spots, and especially over the first two obstacles, increases. Moreover, on the hot top and bottom plates, the vertical temperature gradient for the nanofluid is less than pure fluid which is due to the higher thermal diffusivity of the nanofluid ( $\alpha_{nf}$ ) than the pure fluid ( $\alpha_{bf}$ ). In order to get the better insight of the entropy generation, the constant generated entropy lines, which signify irreversibility of the flow, are also depicted in Fig. 3. As can be understood from this figure, most of the local entropy is generated over plates and obstacles. It is also obvious that as the Reynolds number increases, the constant generated entropy lines are more accumulated especially on obstacles, and as a result, the total entropy generation rate augments through the microchannel.

*4.2. Temperature distribution and velocity profile*

In Fig. 4, the variations of the dimensionless velocity profile and temperature distribution are elucidated in Re =7, Kn = 0.07, and in different volume fraction of nanoparticles. As can be concluded from this figure, augmentation of the volume fraction of nanofluids does not have a significant effect on velocity profile. Regarding the temperature profile, by increasing the volume fraction of nanofluids, the authors are expected the temperature of the nanofluid to reduce; hence, the temperature gradient as well as heat transfer increase. The variations of the dimensionless velocity profile and temperature distribution in  $\phi = 0.03$ , Kn = 0.07 and different Reynolds numbers are displayed in Fig. 5. By increasing the Reynolds number, the velocity profile does not change remarkably; but in center of the microchannel, the temperature of the nanofluid reduces; hence, the temperature gradient, as well as heat transfer, augments. This is because at high Reynolds numbers, the nanofluid does not have sufficient time to contact with hot walls, and as a result, the temperature of the nanofluid decreases.

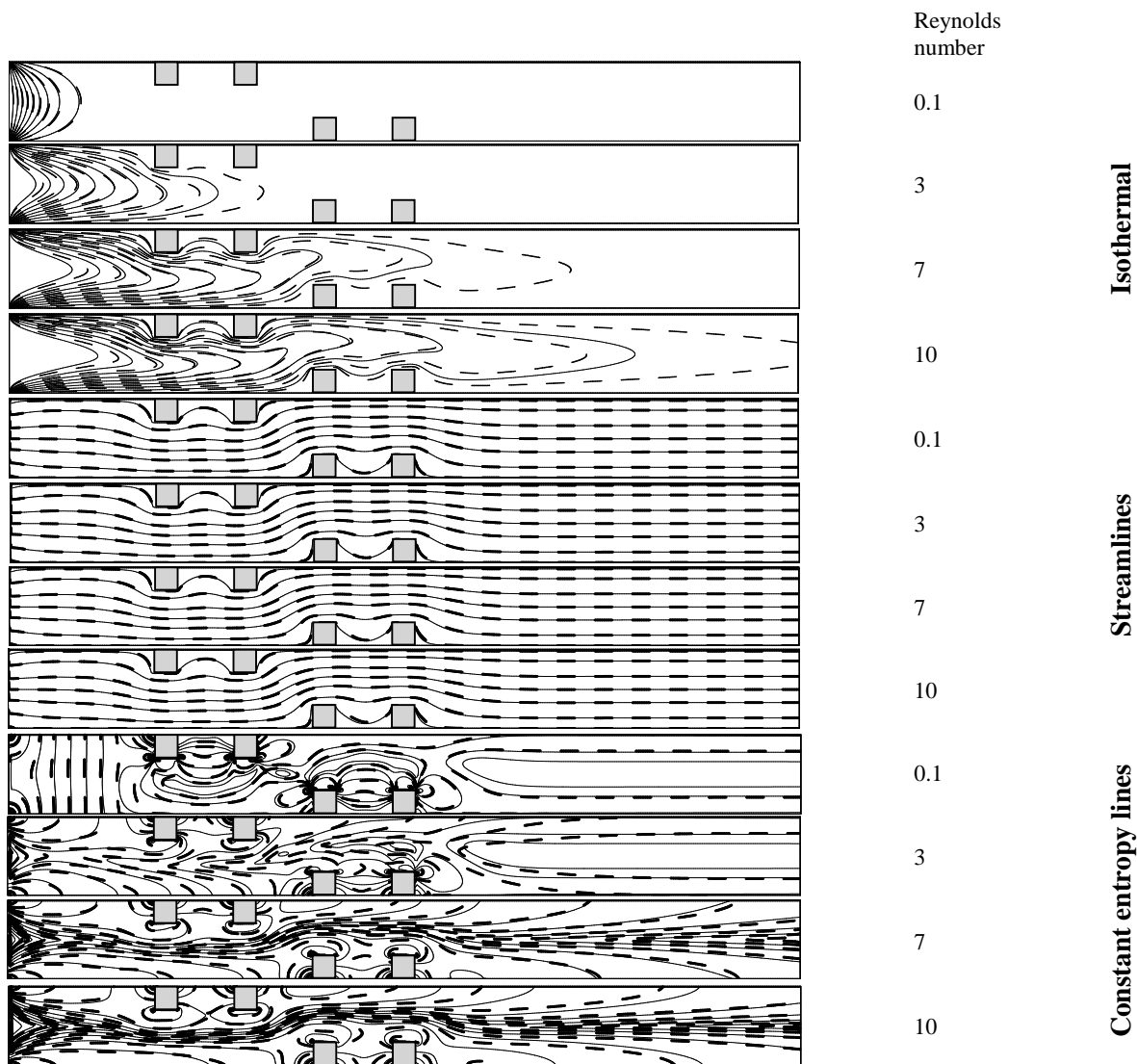


**Fig. 3.** Streamlines, isothermal, and constant generated entropy lines in  $Kn=0.1$ ,  $\phi=0$  (—) and  $\phi=0.03$  (- -) and in different Reynolds numbers.

*4.3. Average Nusselt number and total entropy generation rate*

Figs. 6 and 7 indicate variations of the average Nusselt number and entropy generation rate against the volume fraction at different Reynolds and Knudsen numbers. According to these figures, by increasing the volume fraction of nanoparticles, the average Nusselt number, heat

transfer, and entropy generation increase. Furthermore, with augmentation of the Reynolds number, both of the average Nusselt number and total entropy generation rate increase. What's more, as the Knudsen number increases, the average Nusselt number decreases. Also, when the Knudsen number increases, the total entropy generation rate decreases due to the reduction of the temperature and velocity gradients.

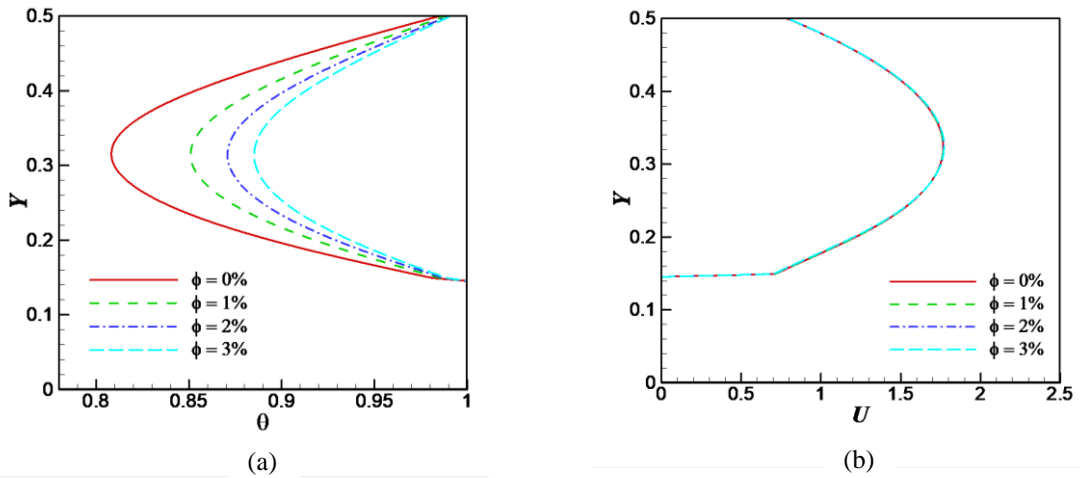


**Fig. 4.** (a): The dimensionless velocity and temperature variations in terms of  $Y$  on micro channel midline in  $Re = 7$ , (b):  $Kn = 0.07$  and different volume fraction of nanoparticles.

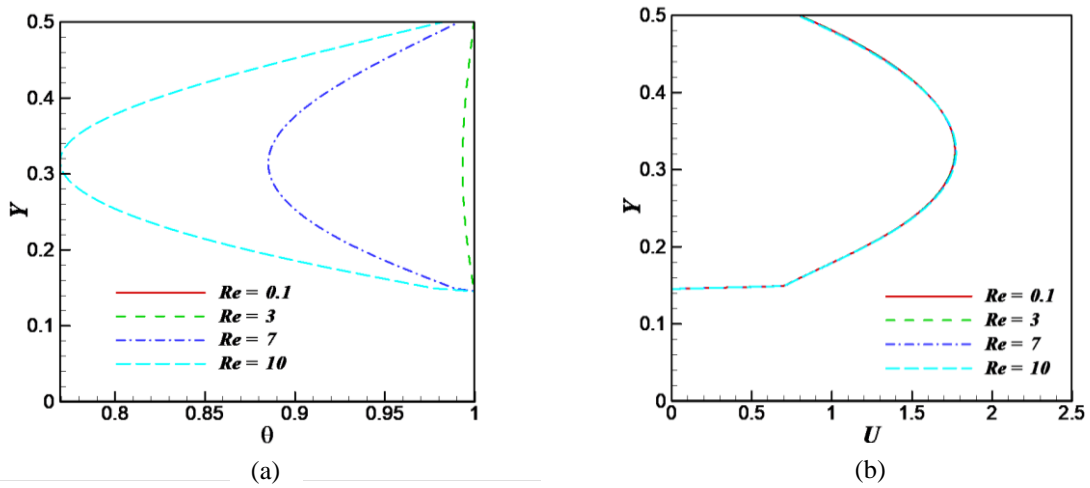


**Fig. 5.** (a) The dimensionless velocity and temperature variations in terms of  $Y$  on microchannel midline in  $\phi = 0.03$ , (b):  $Kn = 0.07$  and different Reynolds numbers.

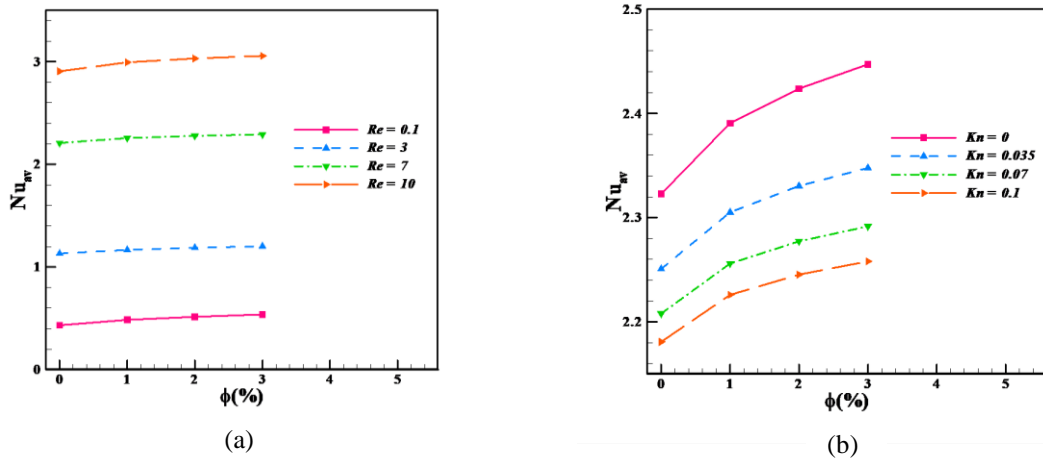


**Fig. 6.** Variation of the average Nusselt number according to the variations of the volume fraction at different (a): Reynolds and (b): Knudsen numbers.

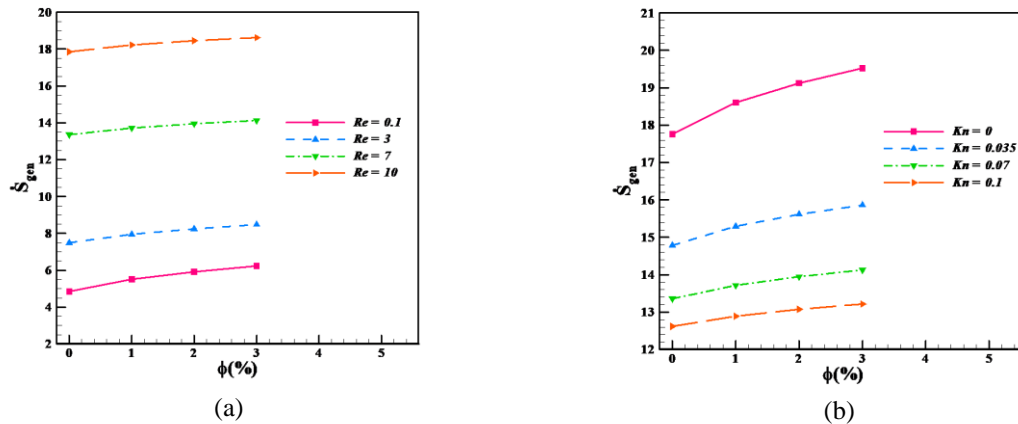


**Fig. 7.** Variation of the entropy generation rate according to the variations of the volume fraction at different (a): Reynolds and (b): Knudsen numbers.

### 5. Conclusions

In this study, flow field, heat transfer, and entropy generation are investigated for forced convection of Cu-water nanofluid in a microchannel. The properties of nanofluid are considered variable with temperature. Moreover, the slip velocity and temperature jump boundary conditions are taken into account in formulating the governing equations. The effects of different parameters such as Reynolds number, the volume fraction of nanoparticles, and Knudsen number on the average Nusselt number and the total entropy generation rate are evaluated. Based on the results:

- Over the top and bottom hot wall, the vertical temperature gradient is very low nearly all over the microchannel, and as a result, the rate of heat transfer is low.
- Augmentation of the volume fraction of nanofluids does not have a significant effect on velocity profile.
- By increasing the Reynolds number, the velocity profile does not change remarkably; but in center of the microchannel, the temperature of the nanofluid reduces; hence, the temperature gradient, as well as heat transfer, augments. This is because, at high Reynolds numbers, the nanofluid does not have sufficient time to contact with hot walls and as a result, the temperature of the nanofluid decreases.

- By increasing the volume fraction of nanoparticles, the average Nusselt number and the total entropy generation augment.
- As the Knudsen number increases, the average Nusselt number decreases.

### Reference

- [1] M. Gad-el-Hak, The fluid mechanics of microdevices: the Freeman scholar lecture, *Journal of Fluids Engineering*, Vol. 121, No. 1, pp. 5-33, (1999).
- [2] A. Beskok, G. E. Karniadakis, Simulation of heat and momentum transfer in complex micro-geometries, *Journal of Thermophysics Heat Transfer*, Vol. 8, No. 4, pp. 355-370, (1994).
- [3] S. Yu and T. A. Ameel, "Slip-flow heat transfer in rectangular microchannels," *International Journal of Heat and Mass Transfer*, Vol. 44, No. 22, pp. 4225-4234, (2001).
- [4] X. Zhu and Q. Liao, "Heat transfer for laminar slip flow in a microchannel of arbitrary cross section with complex thermal boundary conditions," *Applied Thermal Engineering*, Vol. 26, pp. 1246-1256, (2006).
- [5] M. Barkhordari and S. G. Etemad, "Numerical study of slip flow heat transfer of non-Newtonian fluids in circular microchannels," *International*

- Journal of Heat and Fluid Flow*, Vol. 28, No. 5, pp. 1027-1033, (2007).
- [6] S. M. M. Nayinian, M. Shams, H. Afshar, and G. Ahmadi, "Two phase analysis of heat transfer and dispersion of nano particles in a microchannel," in ASME 2008 Heat Transfer Summer Conference collocated with the Fluids Engineering, *Energy Sustainability, and 3rd Energy Nanotechnology Conferences*, pp. 457-463, (2008).
- [7] H. Niazmand, M. Renksizbulut, and E. Saeedi, "Developing slip-flow and heat transfer in trapezoidal microchannels," *International Journal of Heat and Mass Transfer*, Vol. 51, No. 25-26, pp. 6126-6135, (2008).
- [8] K. Hooman, F. Hooman, and M. Famouri, "Scaling effects for flow in micro-channels: variable property, viscous heating, velocity slip, and temperature jump," *International Communications in Heat and Mass Transfer*, Vol. 36, No. 2, pp. 192-196, (2009).
- [9] M. Mollamahdi, M. Abbaszadeh, and G. A. Sheikhzadeh, "Flow field and heat transfer in a channel with a permeable wall filled with  $\text{Al}_2\text{O}_3$ -Cu/water micropolar hybrid nanofluid, effects of chemical reaction and magnetic field," *Journal of Heat and Mass Transfer Research (JHMTR)*, Vol. 3, No. 2, pp. 101-114, (2016).
- [10] G. Sheikhzadeh, A. Aghaei, H. Ehteram, and M. Abbaszadeh, "Analytical study of parameters affecting entropy generation of nanofluid turbulent flow in channel and micro-channel," *Thermal Science*, (2016).
- [11] A. R. Rahmati, A. R. Roknabadi, and M. Abbaszadeh, "Numerical simulation of mixed convection heat transfer of nanofluid in a double lid-driven cavity using lattice Boltzmann method," *Alexandria Engineering Journal*, Vol. 55, No. 4, pp. 3101-3114, (2016).
- [12] D. B. Tuckerman and R. Pease, "High-performance heat sinking for VLSI," *Electron Device Letters, IEEE*, Vol. 2, No. 5, pp. 126-129, (1981).
- [13] S. Yu, and T. A. Ameel, Slip flow heat transfer in rectangular microchannels, *International Journal of Heat and Mass Transfer*, Vol. 44, No. 22, pp. 4225-4234, (2001).
- [14] S. Yu, and T. A. Ameel, Slip-flow convection in isoflux rectangular microchannels, *Journal of Heat Transfer*, Vol. 124, No. 2, pp. 346-355, (2002).
- [15] M. Renksizbulut, H. Niazmand, and G. Tercan, Slip-flow and heat transfer in rectangular microchannels with constant wall temperature, *International Journal of Thermal Science*, Vol. 45, No. 9, pp. 870-881, (2006).
- [16] A. A. Abbasian Arani, M. Abbaszadeh, and A. Ardeshiri, "Mixed convection fluid flow and heat transfer and optimal distribution of discrete heat sources location in a cavity filled with nanofluid," *Transport Phenomena in Nano and Micro Scales*, Vol. 5, pp. 30-43, (2016).
- [17] A. Karimipour, "New correlation for Nusselt number of nanofluid with Ag/ $\text{Al}_2\text{O}_3$ /Cu nanoparticles in a microchannel considering slip velocity and temperature jump by using lattice Boltzmann method," *International Journal of Thermal Sciences*, Vol. 91, pp. 146-156, (2015).
- [18] A. Bejan, Second law analysis in heat transfer, *Energy*, Vol. 5, No. 8-9, pp. 720-732, (1980).
- [19] A. Bejan, *Minimization of Entropy Generation*, CRC Press, Boca Raton, (1996).
- [20] K. Hooman, "Entropy generation for microscale forced convection: effects of different thermal boundary conditions, velocity slip, temperature jump, viscous dissipation, and duct geometry," *international*

- Communications in Heat and Mass Transfer*, Vol. 34, pp. 945-957, (2007).
- [21] O. Haddad, M. Abuzaid, M. Al-Nimr, Entropy generation due to laminar incompressible forced convection flow through parallel-plates microchannel, *Entropy*, Vol. 6, No. 5, pp. 413-426, (2004).
- [22] N. Pourmahmoud, H. Soltanipour, and I. Mirzaee, "The effects of longitudinal ribs on entropy generation for laminar forced convection in a microchannel," *Thermal Science*, pp. 110-110, (2014).
- [23] A. Aghaei, H. Khorasanizadeh, G. A. Sheikhzadeh, and M. Abbaszadeh, "Numerical study of magnetic field on mixed convection and entropy generation of nanofluid in a trapezoidal enclosure," *Journal of Magnetism and Magnetic Materials*, Vol. 403, pp. 133-145, (2016).
- [24] O. Mahian, A. Kianifar, C. Kleinstreuer, A.-N. Moh'd A, I. Pop, A. Z. Sahin, S. Wongwises, A review of entropy generation in nanofluid flow, *International Journal of Heat and Mass Transfer*, Vol. 65, pp. 514-532, (2013).
- [25] F. Oueslati, B. Ben-Beya, "T. Lili, Double-diffusive natural convection and entropy generation in an enclosure of aspect ratio 4 with partial vertical heating and salting sources," *Alexandria Engineering Journal*, Vol. 52, pp. 605-625, (2013).
- [26] Kh. Khanafer, and K. Vafai, A critical synthesis of thermophysical characteristics of nanofluids, *International journal of heat and mass transfer*, Vol. 54, pp. 4410-4428, (2011).
- [27] A. Akbarinia, M. Abdolzadeh, R. Laur, "Critical investigation of heat transfer enhancement using nanofluids in microchannels with slip and non-slip flow regimes," *Applied Thermal Engineering*, Vol. 31, No. 4, pp. 556-565, (2011).

### How to cite this paper:

Majid Kerdarian and Ehsan Kianpour, "Flow field, heat transfer and entropy generation of nanofluid in a microchannel using the finite volume method" *Journal of Computational and Applied Research in Mechanical Engineering*, Vol. 8, No. 2, pp. 211-222, (2018).

**DOI:** 10.22061/JCARME.2018.794

**URL:** [http://jcarme.sru.ac.ir/?\\_action=showPDF&article=998](http://jcarme.sru.ac.ir/?_action=showPDF&article=998)

